



Monte Carlo-based software for 3D personalized dose calculations in image-guided radiotherapy

Coralie Le Derooff, Lucie Berger, Julien Bellec, Guillaume Boissonnat, Hélène Chesneau, Sophie Chiavassa, Julie Desrousseaux, Stephanie Gempp, Olivier Henry, Jimmy Jarril, et al.

► To cite this version:

Coralie Le Derooff, Lucie Berger, Julien Bellec, Guillaume Boissonnat, Hélène Chesneau, et al.. Monte Carlo-based software for 3D personalized dose calculations in image-guided radiotherapy. Physics and Imaging in Radiation Oncology, 2022, 21, pp.108-114. <10.1016/j.phro.2022.02.004>. <hal-03631152v2>

HAL Id: hal-03631152

<https://hal.science/hal-03631152v2>

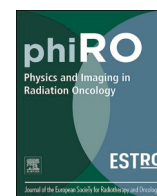
Submitted on 5 Apr 2022

HAL is a multi-disciplinary open access archive for the deposit and dissemination of scientific research documents, whether they are published or not. The documents may come from teaching and research institutions in France or abroad, or from public or private research centers.

L'archive ouverte pluridisciplinaire **HAL**, est destinée au dépôt et à la diffusion de documents scientifiques de niveau recherche, publiés ou non, émanant des établissements d'enseignement et de recherche français ou étrangers, des laboratoires publics ou privés.



Distributed under a Creative Commons CC BY-NC-ND 4.0 - Attribution - Non-commercial use - No Derivative Works - International License



Original Research Article

Monte Carlo-based software for 3D personalized dose calculations in image-guided radiotherapy



Coralie Le Deroff^{a,*}, Lucie Berger^b, Julien Bellec^a, Guillaume Boissonnat^c, H  l  na Chesneau^a, Sophie Chiavassa^d, Julie Desrousseaux^e, St  phanie Gempp^e, Olivier Henry^a, Jimmy Jarri  l^b, Delphine Lazaro^c, Ronan Lefeuvre^a, Vincent Passal^d, Fanny Solinhac^e, Caroline Lafond^{a,f}, Gregory Delpont^d

^a Centre Eug  ne Marquis (Unicancer), Rennes, France

^b Centre Jean Perrin (Unicancer), Clermont Ferrand, France

^c Universit   Paris-Saclay, CEA, List, F-91120 Palaiseau, France

^d Institut de Canc  rologie de l'Ouest (Unicancer), Saint-Herblain, France

^e Assistance Publique – H  pitaux de Marseille, Marseille, France

^f Universit   de Rennes, Inserm, LTSI – UMR 1099, Rennes, France

ARTICLE INFO

Keywords:

IGRT
Monte Carlo dose calculation
Personalized dose
Prostate
Head-and-neck
Breast

ABSTRACT

Background and purpose: Image-guided radiotherapy (IGRT) involves frequent in-room imaging sessions contributing to additional patient irradiation. The present work provided patient-specific dosimetric data related to different imaging protocols and anatomical sites.

Material and methods: We developed a Monte Carlo based software able to calculate 3D personalized dose distributions for five imaging devices delivering kV-CBCT (Elekta and Varian linacs), MV-CT (Tomotherapy machines) and 2D-kV stereoscopic images from BrainLab and Accuray. Our study reported the dose distributions calculated for pelvis, head and neck and breast cases based on dose volume histograms for several organs at risk.

Results: 2D-kV imaging provided the minimum dose with less than 1 mGy per image pair. For a single kV-CBCT and MV-CT, median dose to organs were respectively around 30 mGy and 15 mGy for the pelvis, around 7 mGy and 10 mGy for the head and neck and around 5 mGy and 15 mGy for the breast. While MV-CT dose varied sparsely with tissues, dose from kV imaging was around 1.7 times higher in bones than in soft tissue. Daily kV-CBCT along 40 sessions of prostate radiotherapy delivered up to 3.5 Gy to the femoral heads. The dose level for head and neck and breast appeared to be lower than 0.4 Gy for every organ in case of a daily imaging session.

Conclusions: This study showed the dosimetric impact of IGRT procedures. Acquisition parameters should therefore be chosen wisely depending on the clinical purposes and tailored to morphology. Indeed, imaging dose could be reduced up to a factor 10 with optimized protocols.

1. Introduction

During radiotherapy, frequent in-room imaging sessions are performed to adjust either the patient positioning or the target localization. The so-called image-guided radiotherapy (IGRT), that also includes pre-treatment imaging modalities has offered new treatment opportunities such as toxicity reduction, dose escalation, voxelization or adaptation [1,2]. However, these imaging devices use mostly ionizing radiations and imaging sessions contribute to additional patient irradiation [3].

With IGRT procedures, the healthy volume that receives high doses in the neighborhood of the target volumes may decrease if smaller margins are used [4] or if adaptation is performed to improve targeting [5]. However, the healthy volume that receives low doses may increase due to the larger irradiated volume. Consequently, the imaging dose may increase the risk of late toxicities and therefore needs to be managed.

The American Association of Physicists in Medicine (AAPM) has recently published a report on the management of image guidance doses during radiotherapy, including some general recommendations [6]. One

Abbreviations: IGRT, Image Guided Radiotherapy; MC, Monte Carlo; CBCT, Cone Beam Computed Tomography.

* Corresponding author.

E-mail address: c.lederoff@rennes.unicancer.fr (C. Le Deroff).

<https://doi.org/10.1016/j.phro.2022.02.004>

Received 13 October 2021; Received in revised form 28 January 2022; Accepted 11 February 2022

Available online 26 February 2022

2405-6316/   2022 The Authors. Published by Elsevier B.V. on behalf of European Society of Radiotherapy & Oncology. This is an open access article under the

CC BY-NC-ND license (<http://creativecommons.org/licenses/by-nc-nd/4.0/>).

recommendation consists in communicating the imaging dose associated with IGRT protocols by site (head, thorax, abdomen, pelvis) to physicians. This enables informed decision-making for selecting imaging protocols and ensures that the clinicians are aware of the imaging doses being delivered to their patients [7]. It appears that one must be able to calculate, to optimize and to report additional doses due to IGRT procedures although no dedicated software is yet available in clinical practice [8] and dose optimisation for radiotherapy imaging is not the manufacturer's priority.

The aim of our project was to develop a Monte Carlo (MC) based software able to calculate 3-D personalized in-medium dose distributions based on CT images for the main imaging devices among the manufacturers. The MC models of kV-CBCT systems, stereoscopic systems and a helical MV-CT system have been created and validated [10,11]. The present study, in agreement with AAPM recommendations, reports the dose distributions calculated for three treatment sites (pelvis, head and neck and breast) using three different patient cohorts with various morphologies.

2. Materials and methods

2.1. Monte Carlo based software for personalized dose calculations

A methodology able to compute patient-specific imaging doses on a wide range of IGRT systems and protocols was developed. The methodology was based on MC simulations and we used an in-house modified version of Penelope 2006 [9] that introduced parallelization as specified in [10]. Main IGRT devices were included in the database of the program. For 3D imaging systems, kV-CBCT XVI (Elekta), OBI (Varian) and MV-CT TomoTherapy (Accuray) were modeled. For 2D-kV acquisitions, ExacTrac system (Brainlab) and CyberKnife imaging system (Accuray) were simulated. MC models were previously validated by comparing measurements and simulations in a water phantom and anthropomorphic phantoms [10,11].

In the program workflow, each voxel of the patient CT images was converted into a tissue material with a given atomic composition and density. The conversion was based on Schneider's stoichiometric method [12], where the correspondence between Hounsfield Units (HU) and tissue material was established for various energies (from 80 to 140 kV) for 7 soft tissues and 22 bony tissues, based on CT-HU calibration curves acquired using either a CIRS-062 or a Gammex phantoms. The treatment couch was added to the simulation geometry by a 1.2 g/cm² thick layer of carbon graphite. The imaging isocenter coordinates was chosen along with the imaging protocol by selecting one of the five modelled imaging systems.

The MC simulations were computed on 40 CPUs (Intel Xeon 2,8 GHz E5-2680v2 CPU - Intel Corp., Santa Clara, CA) working in parallel for 2 h in order to obtain 5% dose uncertainty for in-field voxels. The simulation output was an in-medium 3D dose map expressed per primary shower that was converted into an absorbed dose distribution map taking into account the imaging device air Kerma output, the total image charge (mAs), the number of projections and the number of image repetition. The final dose distribution was expressed in dose to medium. The computed dose distribution was saved in Dicom format to be loaded in any usual software for dose evaluation in radiotherapy departments.

2.2. Patient cohorts

Three anatomical sites were selected for this study: the pelvis, the head and neck and the breast. For each site, 15 patients representing a panel of possible morphologies were chosen. A total of 45 patients was evaluated. For the pelvis cohort, only males were included in order to evaluate prostate cancer protocols while for the breast cohort, only females were included to evaluate breast cancer protocols.

All data were anonymized and respected General Data Protection Regulation and local regulations for patient privacy.

2.3. Imaging protocols

The chosen imaging protocol parameters were the most often used in our clinical practice. Parameters are presented in Table 1. Parameters such as mAs per scan may vary from one equipment to another due to provider recommendation and on site dose optimization. The dose output (air Kerma per mAs) for each protocol was measured at the imaging source to axis distance (SAD) using a Farmer ionization chamber.

2.4. Dose for a single imaging session

For each patient over the three cohorts, personalized dose distributions were calculated for a single imaging session for the five modalities. Cumulative dose volume histograms were computed and analysis was performed in terms of median doses (D50%) and dose to 10% of the volume (D10%) for several organs at risk. For each cohort, D50% and D10% statistics included the average, the minimum and the maximum per organ.

2.5. Cumulative imaging dose for daily IGRT

The total additional dose due to in-room imaging was evaluated considering various daily IGRT strategies in terms of imaging modality for different treatment schemes. Given the extreme low doses resulting from a single exposure with 2D-kV imaging modalities (<1 mGy), we have chosen to focus only on 3D imaging modalities and 2D stereotactic imaging involving multiple intra-fraction exposures.

Three particular indications were studied. First, the total imaging dose was assessed for prostate radiotherapy using either XVI-CBCT, OBI-CBCT or MV-CT over 40 sessions. The resulting additional dose for a hypo-fractionated prostate radiotherapy of 5 sessions was also assessed, considering 80 pairs of intra-fraction images per treatment fraction with the CyberKnife system. Secondly, the imaging dose for breast simultaneous integrated boost radiotherapy was assessed considering 28 imaging sessions using either XVI-CBCT, OBI-CBCT or MV-CT as imaging modalities for dose calculations. The results of a head and neck IGRT treatment are presented in Supplementary Material considering 35 imaging sessions.

To calculate the total additional dose, it was assumed that patient position and anatomy were exactly the same over the whole treatment course. Computed dose distributions for a single imaging fraction were multiplied by the total number of acquisitions. Cumulative dose volume histograms were computed and analysis was performed in terms of D50% and D10% of the organ volume, for the selected organs at risk.

3. Results

3.1. Dose for a single imaging session

3.1.1. 3D dose distribution for pelvic cases

kV-CBCT delivered the highest dose among the 5 imaging modalities with a median dose (D50%) of about 15–40 mGy per scan to the bladder, the rectum and the femoral heads, as reported in Table 2. If dose deposition was quite homogeneous between soft tissues, the dose deposition in bony organs was much higher as shown by the dose distributions for the pelvic region in Fig. 1. This effect is inherent to the use of medium energy X-ray sources below 300 keV, due to the important proportion of photoelectric absorption in high Z material. Thus, femoral heads received a dose around 1.5 higher (up to 53 mGy) than the bladder and the rectum.

Note that the difference between XVI and OBI dose was mainly due to the user imaging protocol parameters (higher number of mAs for the XVI than for the OBI, see Table 1).

Important dose differences have been observed among the pelvis cohort due to morphological differences if the same protocol was used for every patient. For example, with the kV-CBCT XVI protocol, the

Table 1

Imaging protocols for three anatomical sites and for five imaging systems. Note the specific parameters for MV-CT imaging with the Tomotherapy: p = pitch (cm), L = acquisition length (cm).

Site	Parameters	kV-CBCT XVI	kV-CBCT OBI	MV-CT Tomotherapy	2D-kV CyberKnife	2D-kV ExacTrac
Pelvis	SAD (cm)	100	100	85	220	223
	kV	120	125	3500	120	120
	Filter	F1	Half fan	/	/	/
	mAs	1690	1080	/	32	51.2
	Scan amplitude	360°	360°	Helical	/	/
	Field size at SAD (cm × cm)	27.7 × 17.8	30.3 × 20.6	40 × 0.4 p = 0.8, L = 12	14.0 × 22.0	12.9 × 12.9
	Air Kerma output at SAD (Gy/mAs or *Gy/min)	4.97 × 10 ⁻⁵	5.58 × 10 ⁻⁵	*1.86 × 10 ⁻²	1.84 × 10 ⁻⁵	1.91 × 10 ⁻⁵
Head and neck	kV	120	100	3500	120	100
	Filter	F1	Full fan	/	None	None
	mAs	264	150	/	20	12.8
	Scan amplitude	360°	200° posterior arc	Helical	/	/
	Field size at SAD (cm × cm)	27.7 × 27.7	22.2 × 16.6	40 × 0.4 p = 0.8, L = 25	14.0 × 22.0	12.9 × 12.9
	Air Kerma output at SAD (Gy/mAs or *Gy/min)	5.17 × 10 ⁻⁵	3.06 × 10 ⁻⁵	*1.86 × 10 ⁻²	1.84 × 10 ⁻⁵	1.25 × 10 ⁻⁵
Breast	kV	120	125	3500	120	120
	Filter	F0	Half fan	/	None	None
	mAs	59.2	270	/	20	51.2
	Scan amplitude	200° posterior arc	360°	Helical	/	/
	Field size at SAD (cm × cm)	27.7 × 27.7	30.3 × 20.6	40 × 0.4 p = 0.8, L = 25	14.0 × 22.0	12.9 × 12.9
	Air Kerma output at SAD (Gy/mAs or *Gy/min)	6.99 × 10 ⁻⁵	5.58 × 10 ⁻⁵	*1.86 × 10 ⁻²	1.84 × 10 ⁻⁵	1.91 × 10 ⁻⁵

Table 2

Median dose (D50%) and D10% values for a single imaging session delivered to several organs at risk (OAR) for the three different anatomical sites investigated using 5 different imaging systems and user-defined imaging protocols (see Table 1). The average, the minimum and the maximum dose values over the cohort are given between brackets for each OAR. For each OAR, the first line is the D50% values and the second line is the D10% values.

Site	OAR	D50% (mGy)	D10% (mGy)			
		kV-CBCT XVI	kV-CBCT OBI	MV-CT TomoTherapy	2D-kV Cyberknife	2D-kV ExacTrac
Pelvis	Bladder	27.6 (20.7; 36.3)	17.7 (12.8; 23.3)	13.4 (12.1; 16.2)	0.22 (0.14; 0.33)	0.27 (0.05; 0.47)
		34.7 (26.9; 43.8)	20.8 (16.1; 26.2)	15.1 (13.5; 16.2)	0.34 (0.24; 0.48)	0.47 (0.14; 0.69)
	Rectum	27.7 (19.0; 33.0)	18.4 (12.5; 22.1)	13.4 (11.9; 14.3)	0.08 (0.04; 0.33)	0.37 (0.28; 0.47)
		32.5 (21.9; 39.6)	20.4 (14.3; 29.9)	14.7 (12.7; 15.6)	0.10 (0.02; 0.16)	0.61 (0.51; 0.79)
	Femoral heads	42.8 (29.2; 53.1)	24.1 (16.6; 30.2)	13.1 (11.8; 14.2)	0.11 (0.06; 0.16)	0.06 (0.03; 0.10)
		68.5 (50.7; 87.5)	37.3 (28.2; 46.2)	15.2 (13.6; 16.0)	0.36 (0.22; 0.45)	0.18 (0.10; 0.31)
Head and neck	Parotids	9.36 (7.20; 10.4)	2.07 (0.60; 2.80)	10.6 (10.1; 11.1)	0.24 (0.21; 0.27)	0.02 (0.01; 0.05)
		10.9 (8.80; 11.8)	2.64 (1.60; 3.50)	11.9 (11.5; 12.3)	0.28 (0.27; 0.32)	0.04 (0.01; 0.07)
	Cochlea	20.9 (18.2; 25.7)	2.54 (0.80; 7.60)	9.40 (8.20; 10.2)	0.37 (0.14; 0.59)	0.04 (0.01; 0.10)
		23.7 (19.9; 29.3)	3.02 (1.00; 8.50)	9.97 (8.71; 10.7)	0.44 (0.18; 0.68)	0.05 (0.02; 0.11)
	Mandible	23.1 (18.0; 25.6)	2.67 (1.40; 3.50)	10.3 (9.78; 10.8)	0.68 (0.35; 0.86)	0.01 (0.01; 0.02)
		33.1 (27.4; 37.0)	5.61 (3.10; 7.10)	11.6 (11.1; 12.0)	0.11 (0.09; 0.13)	0.04 (0.02; 0.07)
Breast	Heart	1.62 (0.90; 2.30)	5.53 (3.60; 8.20)	15.7 (14.0; 18.0)	0.16 (0.10; 0.23)	0.07 (0.03; 0.13)
		2.15 (1.30; 2.90)	7.41 (5.00; 10.5)	17.1 (14.0; 18.0)	0.23 (0.16; 0.31)	0.14 (0.06; 0.23)
	Breasts	1.45 (0.80; 2.10)	4.65 (2.50; 7.70)	16.1 (13.6; 18.5)	0.16 (0.03; 0.34)	0.02 (0.01; 0.03)
		2.16 (1.20; 2.90)	6.18 (3.10; 10.0)	18.9 (16.9; 20.9)	0.30 (0.22; 0.45)	0.03 (0.01; 0.08)
	Lungs	2.33 (1.40; 3.20)	4.75 (2.70; 7.20)	15.9 (13.9; 18.2)	0.08 (0.04; 0.15)	0.09 (0.04; 0.18)
		3.08 (1.90; 4.00)	6.39 (3.40; 9.60)	17.3 (15.2; 19.7)	0.23 (0.09; 0.34)	0.23 (0.13; 0.35)

rectum median dose was 33 mGy for a 74 kg patient compared to 19 mGy for a 131 kg patient (up to 1.75 times more dose).

The dose deposition with MV-CT imaging was homogeneous due to its higher energy (3.5 MV) and only raised slightly at beam intersection due to the helical acquisition mode. For every organ, including bony structures, the median dose was around 15 mGy per acquisition.

The imaging modalities that delivered the lowest dose were the 2D-kV systems from CyberKnife and ExacTrac. Indeed, the dose scale for 2D-kV images was lower than kV-CBCT ones by two orders of magnitude and a pair of images delivered less than 0.5 mGy to each organ. 2D-kV consists in two unique projections, thus there was a steep dose fall-off in the tissues and the highest dose was observed at the beam entrance

being either anterior in case of CyberKnife system (X-ray tubes at the ceiling) or posterior in case of ExacTrac system (X-ray tubes in the ground).

3.1.2. 3D dose distribution for head and neck cases

kV-CBCT and MV-CT acquisitions delivered around 10 mGy to soft tissues while 2D-kV delivered less than 1 mGy as shown in Table 2 by the D50% values to the parotids, the cochlea and to the mandible (average dose of the left and right organs). The dose distribution in the head and neck region (Fig. 2) revealed that important dose deposition occurred in the bony structures (mandible, vertebra and skull) for kV-CBCT and 2D-kV modalities and that vertebra acted as a protector for the medulla due

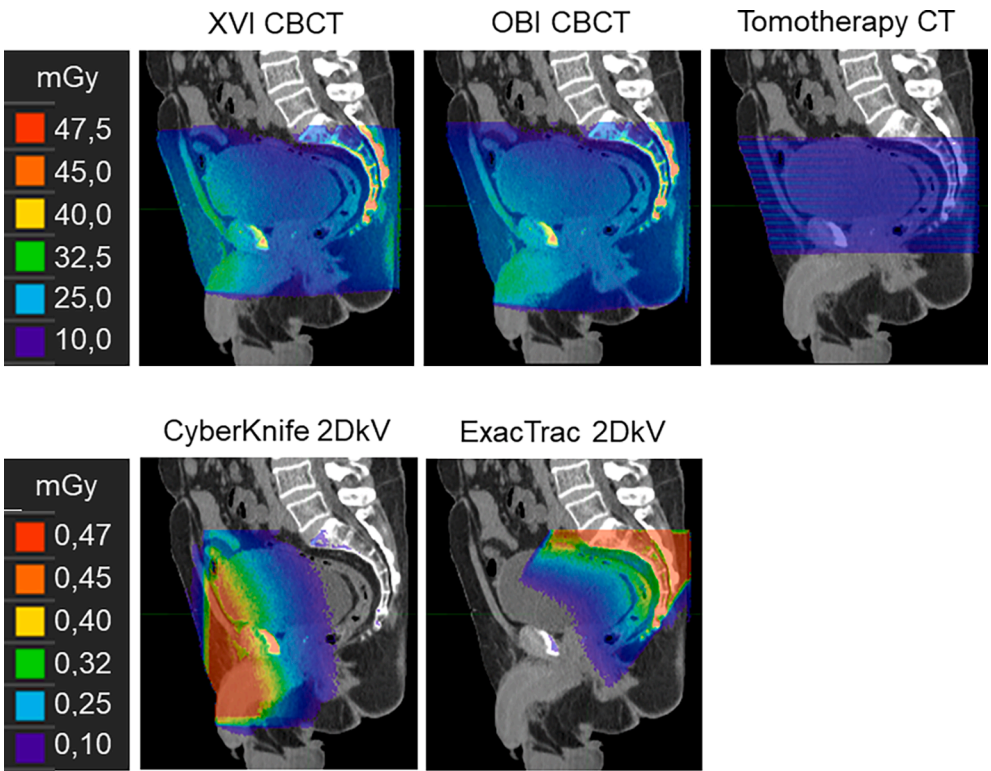


Fig. 1. Dose distributions (mGy) for one imaging session in the pelvic region using 5 different imaging systems and user-defined imaging protocols (see Table 1). The imaging center was central regarding patient anatomy.

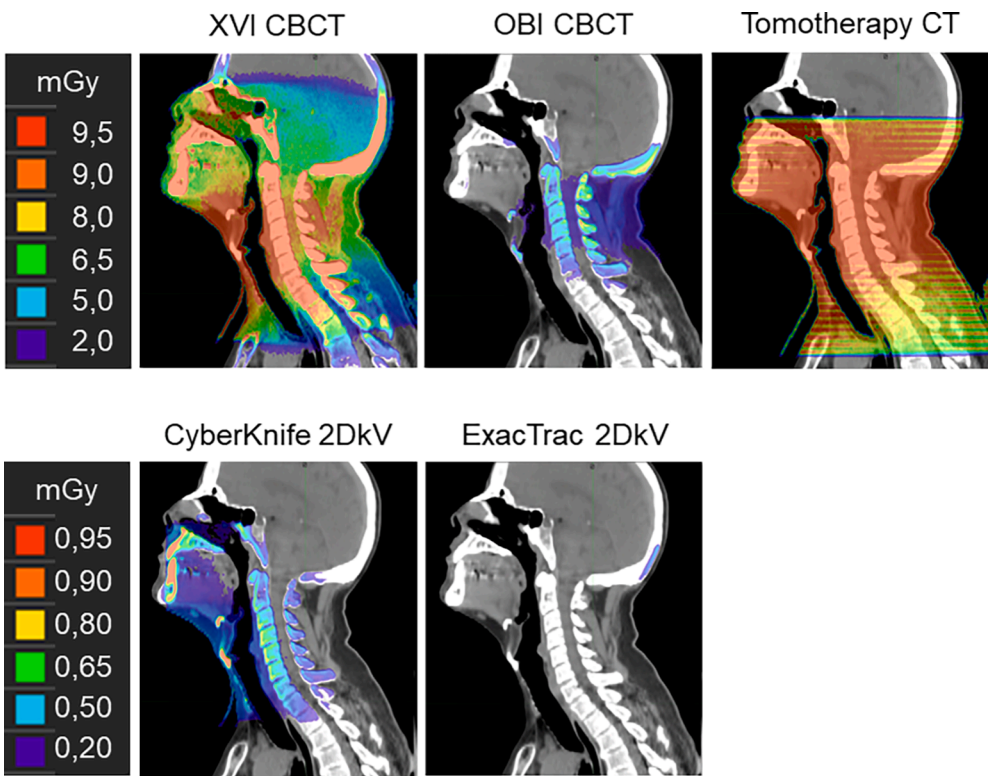


Fig. 2. Dose distribution (mGy) for one imaging session in the head and neck region using 5 different imaging system and user defined imaging protocols (see Table 1). The imaging center was central regarding patient anatomy.

to its high-density composition. The dose has been reduced with user-optimized protocols as shown by the OBI kV-CBCT protocol that delivered up to 12 times less dose than the XVI due to the lower charge (mAs) and the partial posterior acquisition amplitude. Due to lower tube voltage and charge in the imaging protocol, the 2D-kV ExacTrac acquisition delivered much less dose than the CyberKnife one.

3.1.3. 3D dose distribution for thoracic cases

The modality that delivered the highest dose was the MV-CT with around 15 mGy per acquisition for every organ as presented in Table 2 with the D50% values to the heart, the breasts and the lungs (average dose of the left and right organs). For kV-CBCT modalities, the dose levels in soft tissue were lower than 10 mGy and reached around 15 mGy in bones (ribs and vertebra). Depending on the protocol parameters the dose to organs has been reduced to 3 mGy as for the XVI kV-CBCT with reduced mAs and a posterior arc that protects the breasts and lungs as shown in Fig. 3 by the dose distributions in the thoracic region. This user-optimized protocol (using 59.2 mAs) was mainly used for the verification of the patient repositioning when a registration was performed on bones. Besides bones, skin dose was also predominant for 2D-kV images (around 0.6 mGy) while the dose to the heart, breasts and lungs did not exceed 0.3 mGy.

3.2. Cumulative imaging dose for daily IGRT

3.2.1. Imaging dose for prostate IGRT

With daily kV-CBCT the D50% dose value to the bladder and to the rectum was around 1.10 Gy for a 72 kg patient and was significantly higher for the femoral heads (D50% of 1.85 Gy) as shown with the D50% and D10% dose values for each organ at risk in the Supplementary Table A1. The envelope of the DVH over the cohort illustrated the important dispersion due to morphology related to the absorption difference between soft and bony tissues induced by the medium energy beams (<125 keV) as presented in the Fig. 4 a) with the bladder DVH for

the 15 pelvic patient cohort for daily imaging scenarios. The cumulated dose due to 400 intra-fraction image pairs with the CyberKnife system rose to 0.09 Gy (D50% to the bladder) which was close to the dose delivered by one kV-CBCT acquisition. Daily MV-CT resulted in a cumulated D50% value of about 0.53 Gy, that varied sparsely with patient anatomy.

3.2.2. Imaging dose for left breast IGRT

Daily MV-CT resulted in a cumulated D50% value of about 0.45 Gy for the heart, the lungs and the contralateral breast, that varied sparsely with patient anatomy as shown by the DVHs for the heart over the 15 breast patient cohort in case of breast simultaneous integrated boost radiotherapy in 28 sessions and by the D50% and D10% dose values presented in the Supplementary Table A1.

Performing daily kV-CBCT with a full arc (OBI protocol) resulted in a D50% cumulated dose to the heart around 0.15 Gy with a maximum of 0.23 Gy for a skinny patient. The D50% values to the contralateral breast and to the lungs had similar values. Using a posterior semi-arc (XVI protocol) and a lower charge allowed reducing the dose to the heart and to the contralateral breast to a maximum of 0.06 Gy and to the lungs to a maximum of 0.09 Gy.

4. Discussion

2D-kV imaging was by far the modality that delivered the lowest dose to organs with less than 1 mGy per image pair. There was a steep dose fall-off in the tissues but the dose absorption was stronger in bony structure than into soft tissues organs by a factor of 1.7 approximately.

Among 3D modalities, the kV-CBCT delivered higher doses, of about 2–30 mGy per acquisition, depending on the treatment site and the acquisition parameters. Due to the high energy (3.5 MV), the dose distributions delivered by the MV-CT were more homogeneous with lower absorption in the bone but a more important irradiation of the lungs.

The image frequency was of importance and responsible for the

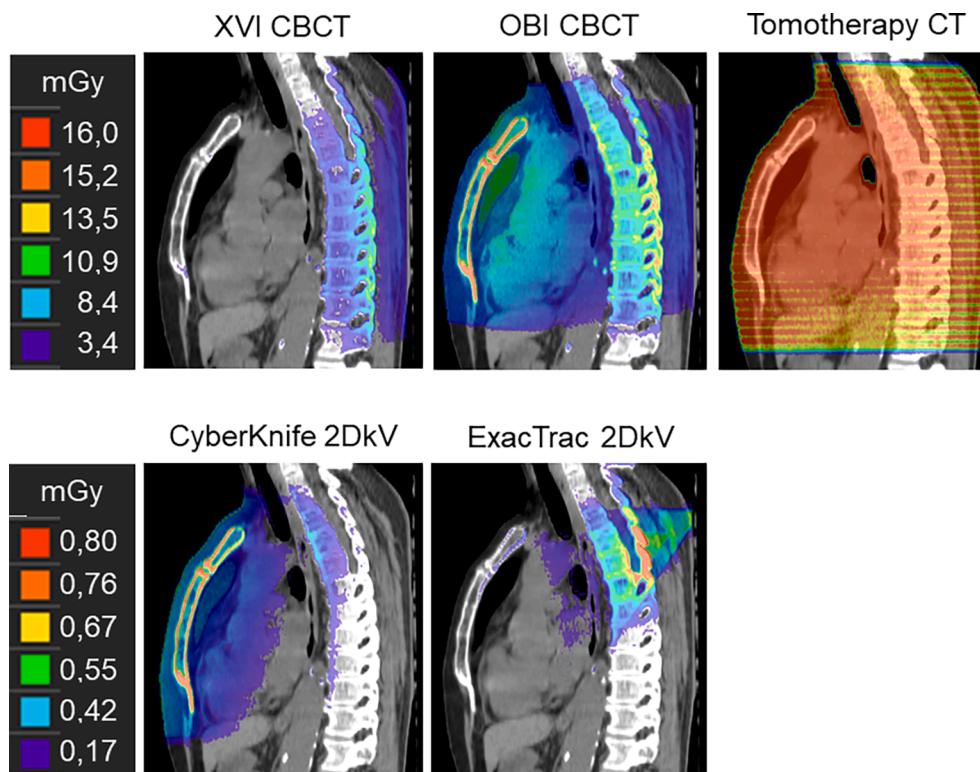


Fig. 3. Dose distribution (mGy) for one imaging session in the thoracic region using 5 imaging system and user defined imaging protocols (see Table 1). The imaging center was central regarding patient anatomy.

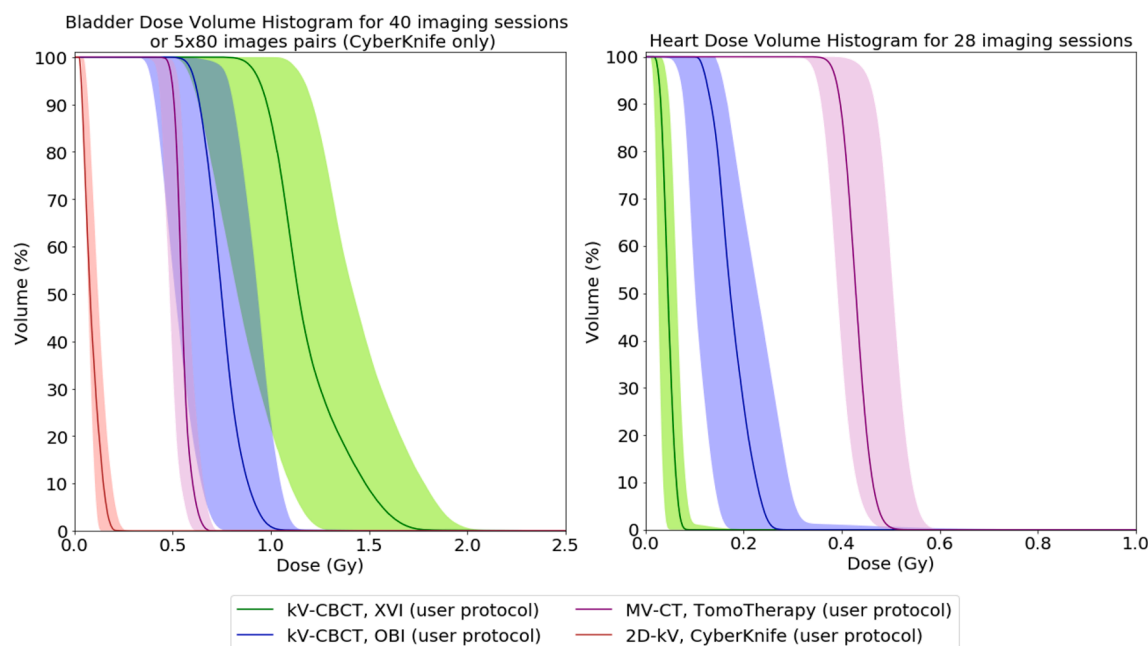


Fig. 4. Envelope dose volume histograms in case of daily IGRT for (a) the bladder in case of normo-fractionated prostate radiotherapy for 3D imaging modalities (40 sessions) and in case of hypo-fractionated radiotherapy performed with 2D-kV stereoscopic imaging (5 sessions) and (b) the heart in case of breast simultaneous integrated boost radiotherapy (28 sessions). The plain curves represent the average DVH and the filled envelope represents all the DVHs over the patient cohort delimited by the cohort extreme values.

accumulated dose to organs if daily and/or intra-fraction images were performed. The AAPM report on image guidance doses (Task Group 180) defines a dose threshold of 5% of the therapeutic target dose, beyond which the additional dose due to imaging was considered significant. The dose distribution over the pelvic cohort showed that daily kV-CBCT along 40 sessions delivered up to 1.7–3.5 Gy to the bladder/rectum and the femoral heads respectively, corresponding respectively to 2.1% and 4.3% of a 80 Gy prostate radiotherapy prescription. This dose levels are in agreement with previous studies [6], and are almost equivalent to an additional treatment session. The dose level for head and neck and thoracic region appeared to be lower than 0.4 Gy for daily imaging. However, the imaging dose should be kept as low as possible by the optimization of the imaging protocols, as long as image quality provides sufficient information for the clinical needs. Besides, for a given image quality, the use of iterative reconstruction algorithms also allows reducing the number of projections or the mAs levels resulting in a reduced dose.

Previous studies reported comparable dose for breast IGRT, varying from 1 to 10 mGy in the heart, breasts and lungs for one kV-CBCT [6,13,14,15]. In agreement with those studies, the different kV-CBCT user protocols in the head and neck and thoracic cohorts of our study showed that reducing the acquisition amplitude from a complete to a partial rotation combined to a reduced charge allowed to preserve organs (breasts for a thoracic CBCT or eyes for head and neck CBCT in case of a posterior arc). Besides, positioning the imaging center in the treated breast contributed to reduce the contralateral breast imaging dose, if permitted by the mechanical limitations of the treatment unit (collision risk between the imaging device and the patient immobilization device) [13].

Protocols should also be adapted to various morphologies [16]. Indeed, the personalized doses from the pelvic cohort stressed the impact of constant parameters used for radically different corpulence (a skinny patient will receive around twice more dose than a very corpulent one). The latest recommendations also suggest to reduce as much as possible the irradiated volume through the field size [6] or by reducing the CBCT angle.

The 3D patient-specific dose levels presented in this study obtained

with our MC based software confirmed that in-room imaging dose values are of importance to initiate their management in clinical practice. The imaging modality and the image frequency should be chosen wisely depending on the clinical needs and the protocols parameters should also be optimized systematically and adapted to morphology. Such broader imaging dose data collection could impulse the definition of dose reference levels in IGRT.

Declaration of Competing Interest

The authors declare that they have no known competing financial interests or personal relationships that could have appeared to influence the work reported in this paper.

Acknowledgments

This work is part of the Additional Imaging Doses – Image Guided Radiation Therapy project (ANR-15-CE19-0009) which is financed by the Agence Nationale de la Recherche.

Appendix A. Supplementary data

Supplementary data to this article can be found online at <https://doi.org/10.1016/j.phro.2022.02.004>.

References

- [1] Jaffray A. Image-guided radiotherapy: from current concept to future perspectives. *Nat Rev Clin Oncol*. 2012;9(12):688–99. <https://doi.org/10.1038/nrclinonc.2012.194>.
- [2] Grégoire V, Guckenberger M, Haustermans K, Lagendijk JJW, Ménard C, Pötter R, et al. Image guidance in radiation therapy for better cure of cancer. *Mol Oncol*. 2020;14(7):1470–91. <https://doi.org/10.1002/mol2.v14.710.1002/1878-0261.12751>.
- [3] De Los Santos J, Popple R, Agazaryan N, Bayouth JE, Bissonnette J-P, Bucci MK, et al. Image guided radiation therapy (IGRT) technologies for radiation therapy localization and delivery. *Int J Radiat Oncol Biol Phys*. 2013;87(1):33–45. <https://doi.org/10.1016/j.ijrobp.2013.02.021>.
- [4] van Herk M. Different styles of image-guided radiotherapy. *Semin Radiat Oncol*. 2007;17(4):258–67. <https://doi.org/10.1016/j.semradonc.2007.07.003>.

- [5] Kron T, Wong J, Rolfo A, Pham D, Cramb J, Foroudi F. Adaptive radiotherapy for bladder cancer reduces integral dose despite daily volumetric imaging. *Radiother Oncol.* 2010;97(3):485–7. <https://doi.org/10.1016/j.radonc.2010.07.023>.
- [6] Ding GX, Alaei P, Curran B, Flynn R, Gossman M, Mackie TR, et al. Image guidance doses delivered during radiotherapy: Quantification, management, and reduction: report of the AAPM Therapy Physics Committee Task Group 180. *Med Phys.* 2018; 45(5):e84–99. <https://doi.org/10.1002/mp.12824>.
- [7] Delpon G, Lazaro D, de Crevoisier R. Management of image guidance doses delivered during radiotherapy. *Cancer Radiother.* 2020;S1278–3218(20): 30324–33. <https://doi.org/10.1016/j.canrad.2020.05.023>.
- [8] Alaei P, Spezi E. Imaging dose from cone beam computed tomography in radiation therapy. *Phys Med.* 2015;31(7):647–58. <https://doi.org/10.1016/j.ejmp.2015.06.003>.
- [9] Francesc S, Fernández-Varea JM, Josep S. PENELOPE-2006: A Code System for Monte Carlo Simulation of Electron and Photon Transport. ISBN: 92-64-02301-1. <https://doi.org/10.1787/9d2cc3d5-en>.
- [10] Boissonnat G, Chesneau H, Barat E, Dautremere T, Garcia-Hernandez J-C, Lazaro D. Validation of histogram-based virtual source models for different IGRT kV-imaging systems. *Med Phys.* 2020;47(9):4531–42. <https://doi.org/10.1002/mp.v47.910.1002.mp.14311>.
- [11] Passal V, Boissonnat G, Chiavassa S, Lazaro D, Delpon G. Monte Carlo calculation of absorbed doses due to imaging sessions delivered to patients during Tomotherapy Image-Guided Radiotherapy courses. *International Conference on Monte Carlo Techniques for Medical Applications 2017*. https://agenda.infn.it/event/12594/attachments/11021/12382/International_Conference_on_Monte_Carlo_Techniques_for_Medical_Applications_MCMA2017_-_Book_of_abstracts.pdf.
- [12] Schneider U, Pedroni E, Lomax A. The calibration of CT Hounsfield units for radiotherapy treatment planning. *Phys Med Biol.* 1996;41(1):111–24. <https://doi.org/10.1088/0031-9155/41/1/009>.
- [13] Alvarado R, Booth JT, Bromley RM, Gustafsson HB. An investigation of image guidance dose for breast radiotherapy. *J. Appl. Clin. Med. Phys.* 2013;14(3):25–38. <https://doi.org/10.1120/jacmp.v14i3.4085>.
- [14] Stelczer G, Tatai-Szabó D, Major T, Mészáros N, Polgár C, Pálvölgyi J, et al. Measurement of dose exposure of image guidance in external beam accelerated partial breast irradiation: evaluation of different techniques and linear accelerators. *Phys. Med* 2019;63:70–8. <https://doi.org/10.1016/j.ejmp.2019.05.020>.
- [15] Sun W, Wang B, Qiu Bo, Liang J, Xie W, Deng X, et al. Assessment of female breast dose for thoracic cone-beam CT using MOSFET dosimeters. *Oncotarget* 2017;8(12): 20179–86.
- [16] Wood TJ, Moore CS, Horsfield CJ, Saunderson JR, Beavis AW. Accounting for patient size in the optimization of dose and image quality of pelvis cone beam CT protocols on the Varian OBI system. *Br J Radiol.* 2015;88(1055):20150364. <https://doi.org/10.1259/bjr.20150364>.